Lkb1 Deficiency Causes Prostate Neoplasia in the Mouse

Helen B. Pearson,[1] Afshan McCarthy,[2] Christopher M.P. Collins,[3] Alan Ashworth,[2] and Alan R. Clarke[1]

[1]Cardiff University, School of Biosciences, Cardiff, Wales, United Kingdom; [2]Breakthrough Breast Cancer Research Center, The Institute of Cancer Research, London, United Kingdom; and [3]Bristol Royal Infirmary, Department of Pathology, Bristol, United Kingdom

Abstract

Mutation of *LKB1* is the key molecular event underlying Peutz-Jeghers syndrome, a dominantly inherited condition characterized by a predisposition to a range of malignancies, including those of the reproductive system. We report here the use of a *Cre-LoxP* strategy to directly address the role of Lkb1 in prostate neoplasia. Recombination of a *LoxP*-flanked *Lkb1* allele within all four murine prostate lobes was mediated by spontaneous activation of a *p450 CYP1A1*-driven *Cre recombinase* transgene (termed *AhCre*). Homozygous mutation of *Lkb1* in males expressing *AhCre* reduced longevity, with 100% manifesting atypical hyperplasia and 83% developing prostate intraepithelial neoplasia (PIN) of the anterior prostate within 2 to 4 months. We also observed focal hyperplasia of the dorsolateral and ventral lobes (61% and 56% incidence, respectively), bulbourethral gland cysts associated with atypical hyperplasia (100% incidence), hyperplasia of the urethra (39% incidence), and seminal vesicle squamous metaplasia (11% incidence). PIN foci overexpressed nuclear β-catenin, p-Gsk3β, and downstream Wnt targets. Immunohistochemical analysis of foci also showed a reduction in Pten activation and up-regulation of both p-PDK1 (an AMPK kinase) and phosphorylated Akt. Our data are therefore consistent with deregulation of Wnt and phosphoinositide 3-kinase/Akt signaling cascades after loss of Lkb1 function. For the first time, this model establishes a link between the tumor suppressor Lkb1 and prostate neoplasia, highlighting a tumor suppressive role within the mouse and raising the possibility of a similar association in the human. [Cancer Res 2008;68(7):2223–32]

Introduction

Prostate cancer is the second most common malignancy next to lung cancer in men (1). A central limitation to studying prostate cancer has been the lack of suitable animal models that recapitulate all the stages of human disease progression. This has at least in part been alleviated by the generation of a range of mouse strains with prostate phenotypes, including those mutant for RB, PTEN, AR, AKT, and, more recently, β-catenin (2). However, it remains of paramount importance to develop novel models of prostate cancer to further our understanding of the molecular mechanisms and genetic events underlying prostate cancer.

LKB1 encodes a serine-threonine kinase that was first identified as a gene whose multiple germ line mutations abrogate enzymatic function and are associated with familial Peutz-Jeghers syndrome (PJS; ref. 3). The disorder is characterized by melanin deposits on the buccal mucosa, lips, and digits and the risk of intestinal hamartomas and extraintestinal cancers, such as stomach, pancreas, thyroid, and those of the reproductive organs is at least 10-fold higher than the general population (4). The molecular mechanisms underlying this enhanced tumor predisposition remain to be fully elucidated, but LKB1 has been implicated in the regulation of multiple pathways associated with tumor prevention (3–7). These include chromatin remodeling, angiogenesis, p53-dependent apoptosis, cell cycle arrest, energy metabolism, fatty acid biosynthesis, Wnt signaling, proliferation, polarity, and differentiation (4, 8–11). Recently, somatic deletion of *Lkb1* has been linked to lung tumorigenesis and mutation screening of human lung cancer patients revealed *LKB1* inactivation is a common event in lung adenocarcinomas (34%) and squamous cell carcinomas (19%), further implicating Lkb1 as a tumor suppressor (12). In addition, somatic mutation of *Lkb1* has been reported in pancreatic and biliary cancers (13), as well as malignant melanomas (14).

LKB1 is a member of the Snf1 family of kinases and has been shown to phosphorylate at least 13 members of the AMPK subfamily, many of which play a fundamental role in metabolic regulation (7). In particular, Lkb1 can activate AMPK by phosphorylating Thr^{172} within the T-loop (11, 15). This leads to mTOR inhibition via TSC2 (tuberin) to suppress cell growth and proliferation (16), as well as down-regulating fatty acid and cholesterol biosynthesis and enhancing glucose uptake and glycolysis (17, 18). However, to date, there is little published data to support a direct role for AMPK deregulation in prostate tumorigenesis (19).

With respect to the Wnt pathway, it has been reported that loss of function of LKB1 elevates Wnt signaling via its regulation of MARK3 (Par1A, cTAK). In the absence of Lkb1, Par1A is unphosphorylated and available to participate in the Wnt cascade, instigating translocation of β-catenin into the nucleus where it instructs transcription of target genes to stimulate proliferation (8). This gives a direct mechanism, whereby mutation of LKB1 may lead to activated Wnt signaling. The potential relevance of such deregulation to prostate cancer has been indicated through studies of human prostate cancer that have identified both mutations in *β-catenin* and aberrant β-catenin expression (20). Further evidence in support of such a link is derived from Cre-Lox–based models, which develop high-grade PIN and squamous metaplasia after Cre-mediated activation of a constitutive β-catenin mutation (20, 21). Most recently, the rat probasin promoter (*PB-Cre4*) has been used to drive *Cre*-mediated deletion of *Apc* in the prostate, and this has been shown to predispose to adenocarcinoma of the prostate (22).

LKB1 has also been shown to interact with the tumor suppressor PTEN and thereby the phosphoinositide 3-kinase (PI3K)/Akt and mTOR pathways. The most direct evidence for this interaction was

Requests for reprints: Alan Clarke, University of Cardiff, Museum Avenue, Cardiff, South Glamorgan, CF10 3US, United Kingdom. Phone: 44-0-2920-879115; Fax: 44-02920 874116; E-mail: Clarkear@cardifff.ac.uk.

doi:10.1158/0008-5472.CAN-07-5169

derived from *in vitro* studies that have shown LKB1 to bind and phosphorylate PTEN (3, 23). This interaction has been speculated to result in PTEN stabilization and activation (23). Further indirect evidence for an interaction comes from the observation that ~70% of PJS patients also harbor mutation or display loss of at least one allele of *PTEN* (24). Any potential interaction between PTEN and LKB1 is of particular relevance to prostate neoplasia, as PTEN is well established as a tumor suppressor within this tissue. In humans, *PTEN* has been reported to be frequently deleted in prostate adenocarcinomas (24). In mice, homozygous inactivation of *Pten* leads to embryonic lethality (25), whereas heterozygosity predisposes to prostate carcinoma within 9 to 16 months (50%). This phenotype can be accelerated by additional homozygous deletion of *Cdkn1b*, with carcinomas occurring within 3 months on this background (26). Prostate-specific deletion of *Pten* has also been achieved using the *PB-Cre4* construct to drive recombination of a LoxP-flanked *Pten* allele. This model recapitulates the full spectrum of human prostate cancer progression from hyperplasia, low-grade PIN, high-grade PIN, carcinoma, and metastasis (27). Finally, it has also been argued that progressive depletion of *Pten* levels correlates with a more aggressive prostate phenotype and elevated Akt signaling (24), frequently associated with human prostate cancer (28).

There is currently little in the literature to directly link *LKB1* mutation with human or murine prostate neoplasia. However, the fact that somatic LKB1 mutations have been observed in human lung cancer and the observation of Lkb1-driven lung tumorigenesis in the mouse suggests that Lkb1 may have a broad tumor suppressive role in epithelial tissues (12).

In the prostate, LKB1 protein has been detected in the cytoplasm of luminal cells using immunohistochemistry (29) and low levels of *Lkb1* mRNA are detectable (30). Sequencing studies have reported that *LKB1* is mutated in one of five sequenced human prostate carcinoma cell lines, with a frame-shift deletion (p.K178fs*86) within the kinase domain of DU145 cells (31). Further support for a tumor suppressive role for Lkb1 comes from a whole-genome scan study that identified an association between chromosome segments 19q12-q13.11 and prostate cancer aggressiveness (32). The chromosome segment 19p13.3 harbors the LKB1 tumor suppressor gene and also contains members of the kalikrein family (such as KLK3, PSA) and the *MUC16* gene that encodes the ovarian cancer antigen CA125 (32). Deletions, amplifications, and structural rearrangements of chromosome 19 have also been reported in a variety of tumors, including pancreatic adenocarcinomas, both benign and anaplastic thyroid tumors and stomach cancers (reviewed in ref. 32). Interestingly, prostate cancer has also been anecdotally reported in a PJS patient (66 years old) after the development of colon cancer (6). The presence of prostate cancer in PJS patients is not a frequent occurrence, possibly as a consequence of the normal age of onset of disease. Prostate cancer is typically diagnosed in the seventh decade of life, whereas PJS patients have an average life span of 57 years (4).

Together with the biochemical evidence of pathway interaction, these observations suggest a potential role for deregulated LKB1 signaling in prostate cancer. To directly assess this possibility *in vivo*, we have characterized the phenotype of mice deficient for *Lkb1* within the prostate. Mice engineered to carry floxed (fl) *Lkb1* alleles ($Lkb1^{fl/fl}$; ref. 33), where the kinase domain has been replaced by a cDNA cassette encoding exons 5 to 7, enabled *Lkb1* deletion within the prostate by using the *AhCre* promoter to drive expression of *Cre* recombinase (34). By applying this strategy, we show that loss of *Lkb1* predisposes to atypical hyperplasia (AH) that progressed to PIN in the anterior lobe and focal hyperplasia associated with nuclear atypia of the dorsolateral and ventral lobes within 2 to 4 months. Within PIN lesions, we observe elevation of both the PI3K/Akt and Wnt signaling pathways, supporting the concept that loss of *Lkb1* promotes neoplasia through deregulation of these pathways.

Materials and Methods

Generation of $AhCre^{+}Lkb1^{fl/fl}$ mice. All animal studies and breeding were carried out under a UK Home Office project license. $Lkb1^{fl/fl}$ mice and the *AhCre* transgenic mice have been described previously (33, 34). The *Lkb1* and *AhCre* alleles were backcrossed six times onto a C57BL/6 background. Mice containing one wild-type *Lkb1* allele and one floxed allele ($Lkb1^{+/fl}$) were mated with *AhCre*-positive mice carrying the *Rosa26* reporter allele (35). The *Lkb1* heterozygous progeny from this cross was intercrossed to generate $AhCre^{+}Lkb1^{fl/fl}$ mice (as $Lkb1^{fl/fl}$ males are sterile; ref. 33). Cohorts were aged, and the male genitourinary (GU) tract was harvested when mice developed symptoms. Mice were genotyped by PCR using DNA isolated from tail biopsies. The wild-type and LoxP-flanked *Lkb1* alleles were detected using the primers *Lkb1fwd*, 5′-GATTTCCGCCAGCTGATTGA-3′ and *Lkb1rev*, 3′-AGTGTGACCCCAGCTGACCA-5′ producing 320-bp (wild-type) and 280-bp (floxed) PCR fragments. Recombined *Lkb1* was detected using *Lkb1rec1* 5′-CAGAATCACATCCCCTGGTT-3′ and *Lkb1rec2*, 3′-TTCCCCTCCTCCTGCTAGAT-5′, producing a PCR product of 500 bp. *Cre recombinase* activity was induced in control mice by four i.p. injections of 80 mg/kg β-naphthoflavone within 24 h. Recombined liver tissue was harvested 7 d later.

β-Galactosidase analysis. To determine the pattern of recombination at the *Rosa26R* reporter locus, sectioned material was analyzed as previously described, except X-gal staining was reduced to 1 h at 37°C (34).

Tissue isolation. Tissue was harvested as described previously (36) and fixed for no longer than 24 h in 10% neutral buffered formaldehyde at 4°C before being embedded in paraffin and sectioned at 5 μm. Frozen sections were prepared by snap-freezing in liquid nitrogen, embedded in OCT on dry ice, and sectioned at 10 μm.

Histology, immunohistochemistry, and immunofluorescence. For histology, sections were stained with H&E. For immunohistochemistry, antigen retrieval was performed by incubating the slides in 1× citrate buffer (pH 6.0) in the microwave on full power for 15 min, and endogenous peroxidase activity was inactivated in a solution containing 1.5% H_2O_2 in deionized water. Detection and visualization was carried out using the 3,3′-diaminobenzidine chromagen (DAKO Cytomation) according to the manufacturer's protocol. Images were taken at 40× magnification using "AnalySIS" software (Olympus Soft Imaging System GMBH)", and scale bars were added to represent 50 μm. Control slides known to be positive for each antibody were incorporated. Primary antibodies were obtained from the following sources: anti-androgen receptor 1:100 dilution (Lab Vision Corporation), anti–β-catenin 1:50 dilution (Transduction Laboratories), CD44 1:50 dilution (PharMingen), anti-Foxa1 1:800 dilution (Clone 2F83, Seven Hills Bioreagents), anti-pGsk3β (Ser^{9}) 1:50 dilution (Cell Signaling Technology), anti–Keratin-5 1:1000 dilution (Covance), anti–Ki-67 1:200 dilution (Vector Laboratories), anti-p63 1:50 dilution (Lab Vision Corporation), anti–p-PTEN (Ser^{380}/$Thr^{382/383}$) 1:25 dilution (Cell Signaling Technology), anti-PTEN 1:100 dilution (Cell Signaling Technology), anti–p-AKT (Ser^{473}) 1:50 dilution (Cell Signaling Technology), anti-PDK1 (Ser^{241}) 1:50 dilution (Abcam), anti–Keratin-18 1:20 dilution (Progen), anti–p-AMPK (Thr^{172}) 1:50 dilution (Cell Signaling Technology), anti–p-mTOR (Ser^{2448}) 1:100 dilution (Cell Signaling Technology), anti–p-p70-S6K (Thr^{421}/Ser^{424}) 1:100 dilution (Cell Signaling Technology), and anti–p-S6 ribosomal protein (p-Rps6; $Ser^{240/244}$) 1:100 dilution (Cell Signaling Technology).

For immunofluorescence, the frozen sections were treated with pepsin solution (Zymed) and incubated with the primary rabbit polyclonal anti–zona occludens 1 (ZO-1) antibody 1:20 dilution (Zymed). The primary was detected using the AlexaFluor-488 Nanogold Fab fragment of goat anti-rabbit

IgG (Molecular Probes) 1:200 dilution. Slides were mounted with Vectashield HardSet + 4′,6-diamidino-2-phenylindole mounting medium (Vector Laboratories), and fluorescence was detected using the *Leica TCS SP2 AOBS* confocal microscope.

***In situ* hybridization.** The Qiagen midi-prep kit was used to produce large-scale preparation of the *Lkb1* insert, an *Lkb1* full-length cDNA clone inserted in the *pYX-Asc* vector (IRAVp968E05123D, RZPD). Templates were prepared by linearization with *Eco*R1 or *Not*1 (Promega); DNA phenol chloroform was extracted, and ethanol was precipitated. The plasmid sequence was checked by automated sequencing, confirming 100% identity of the *Lkb1* clone with the National Center for Biotechnology Information Sequence (accession number BC052379). Anti-sense and sense RNA probes were then obtained by *in vitro* transcription using T3 and T7 RNA polymerases (Roche) and labeled using the DIG RNA labeling kit (BM 1175025, Roche). *In situ* hybridization was carried out as described previously on 10% formalin-fixed paraffin-embedded sections (37). Briefly, sections were fixed in 4% paraformaldehyde at 4°C for 15 min, treated with proteinase K (20 mg/mL), and hybridized with the probes overnight at 65°C. The sections were washed at 65°C and adsorbed with alkaline phosphatase-conjugated anti-DIG antibody (Roche) overnight at 4°C. Alkaline phosphatase activity was detected by using BM purple AP solution (Roche).

Laser capture microdissection and DNA isolation and amplification. Frozen tissue was sectioned (at 15–20 μm) onto polyethylene naphthol membrane-coated glass slides (PALM Microlaser Technologies) and lightly stained with 1% cresyl violet acetate. Laser capture microdissection (LCMD) was performed immediately and did not exceed 30 min. DNA was isolated with the QIAamp DNA microkit (Qiagen) and amplified using the Genomiphi DNA amplification kit (Amersham). PCR reactions were performed in the log phase of amplification using 100 ng of LCMD–amplified DNA in a 50-μL reaction.

Results

AhCre$^+$Lkb1$^{fl/fl}$mice have a reduced life span. *AhCre*$^+$ mice were intercrossed with mice carrying a LoxP-flanked *Lkb1* allele and the *Rosa26* reporter allele. Cohorts of *wild-type* (*AhCre*$^+$-*Lkb1*$^{+/+}$), *AhCre*$^+$*Lkb1*$^{+/fl}$ *AhCre*$^-$*Lkb1*$^{fl/fl}$, and *AhCre*$^+$*Lkb1*$^{fl/fl}$ mice were generated and aged. Each cohort contained a minimum of 20 males. Animals were then monitored for signs of illness and killed when they became symptomatic of disease (Fig. 1*A*). *Wild-type, AhCre*$^+$*Lkb1*$^{+/fl}$, and *AhCre*$^-$*Lkb1*$^{fl/fl}$ cohorts showed average survival times exceeding 450 days and did not significantly differ from each other (χ^2 test). However, all *AhCre*$^+$*Lkb1*$^{fl/fl}$ mice became ill by 200 d, with a significantly reduced average survival of 83 d compared with *wild-type* ($P < 0.0001$, $\chi^2 = 39.85$).

***AhCre*$^+$*Lkb1*$^{fl/fl}$ mice develop multiple GU phenotypes, including *PIN*.** Histologic analysis of the GU tract was performed in accordance with the consensus report from the Bar Harbor meeting of the mouse models of human cancer consortium prostate pathology committee (36). No gross phenotype was observed in *wild-type* ($n = 21$), *AhCre*$^+$*Lkb1*$^{+/fl}$ ($n = 18$), and *AhCre*$^-$*Lkb1*$^{fl/fl}$ ($n = 19$) mice, whereas the *AhCre*$^+$*Lkb1*$^{fl/fl}$ cohort ($n = 20$) was predisposed to a number of GU phenotypes.

The anterior prostate from *AhCre*$^+$*Lkb1*$^{fl/fl}$ mice between 2 to 4 months of age revealed atypical hyperplastic foci (100% incidence) and progression to prostate neoplasia predominantly in the proximal region of the duct (Fig. 2*A*). PIN was observed as early as 8 weeks when mice became sick (83% incidence). Within these lesions, solid and cribriform intraluminal proliferation of markedly atypical epithelial cells was accompanied by cytologic (nuclear) atypia, such as nuclear enlargement, pleomorphism, chromatin abnormalities, and an increased prominence of nucleoli, along with apparent focal rosetting that contained mitotic bodies (38). This process was also coupled to thickened stroma surrounding the acini and scattered interstitial infiltrate of lymphocytes and plasma cells. Sparse lymphocytes were also observed within some AH and PIN lesions and in severe cases obstructing prostate acini, resulting in gross tubular dilation. Dorsolateral and ventral lobes displayed a less severe phenotype, where cells exhibited nuclear atypia associated with focal epithelial hyperplasia with 61% and 56% incidence, respectively (Fig. 2*B*).

In addition to PIN, *AhCre*$^+$*Lkb1*$^{fl/fl}$ mice displayed other GU phenotypes. The cohort could be identified visually from 6 to 8 weeks of age because 100% of the mice developed swellings at the base of the tail. Histologic analysis from this region revealed bulbourethral gland (BUG) cysts associated with atypical hyperplasia (Fig. 2*C*). The acinar mucosal epithelium of these cysts was characterized by a loss of cell polarity and was composed primarily of ductal cells, consistent with reduced secretory function indicative of the depleted foamy cytoplasm, similar to an Nkx3.1 deficiency (39, 40). The presence of interstitial, AH, and PIN inflammatory cells is probably linked to disruption of the cystic BUGs. It is unlikely that the inflammation predisposes to the prostate phenotype, because lesions were not regenerative. We also identified urethral gland hyperplasia in 39% of *AhCre*$^+$*Lkb1*$^{fl/fl}$ mice (Fig. 2*Di,ii*). Nodular hyperplasia of the membranous urethra transitional epithelium (UGH) within the lamina propria and a predisposition to cytologic atypia was apparent. There were also two cases (11%) of seminal vesicle squamous metaplasia (SV SqM; Fig. 2*Diii-iv*). Interestingly, somatic mutation of *Lkb1* in the lung has been shown to predispose to squamous metaplasia (12). Finally, all *Lkb1*$^{fl/fl}$ mice were sterile, correlating with previous reports (33). PIN is not a likely cause of our observed reduced longevity. Health of the *AhCre*$^+$*Lkb1*$^{fl/fl}$ male cohort deteriorated, owing to a combination of phenotypes. These include the development of both cystic BUGs (susceptible to rupture) and subsequent infection

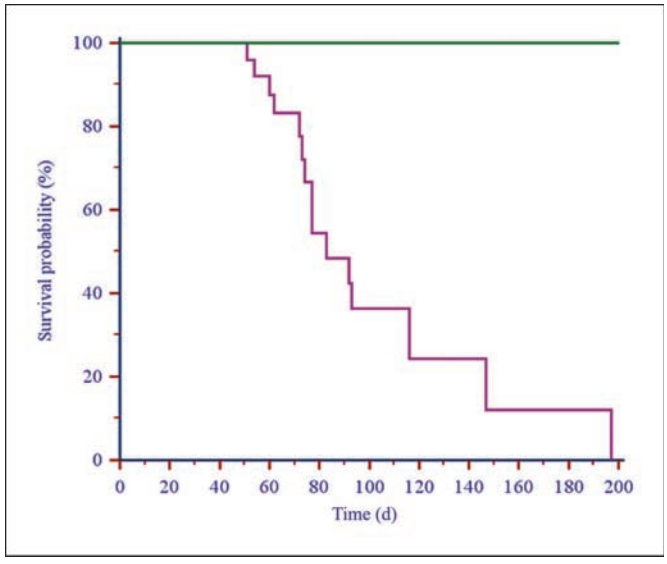

Figure 1. *AhCre*$^+$*Lkb1*$^{fl/fl}$ male mice display reduced longevity. Kaplan-Meier plot of the *AhCre*$^+$*Lkb1*$^{+/+}$ ($n = 26$), *AhCre*$^+$*Lkb1*$^{fl/+}$ ($n = 41$), *AhCre*$^-$*Lkb1*$^{fl/fl}$ ($n = 20$) cohorts were all represented in green, and *AhCre*$^+$*Lkb1*$^{fl/fl}$ mice ($n = 26$) were illustrated in purple. *AhCre*$^+$*Lkb1*$^{fl/fl}$ mice show decreased longevity, where 100% of the cohort did not survive past 200 d. χ^2 tests confirmed *AhCre*$^+$*Lkb1*$^{fl/fl}$ mice exhibit a significantly reduced average survival of 83 d compared with *wild-type* ($P < 0.0001$, $\chi^2 = 39.85$), *AhCre*$^+$*Lkb1*$^{+/fl}$ ($P < 0.0001$, $\chi^2 = 59.01$), and *AhCre*$^-$*Lkb1*$^{fl/fl}$ ($P < 0.0001$, $\chi^2 = 31.97$) cohorts.

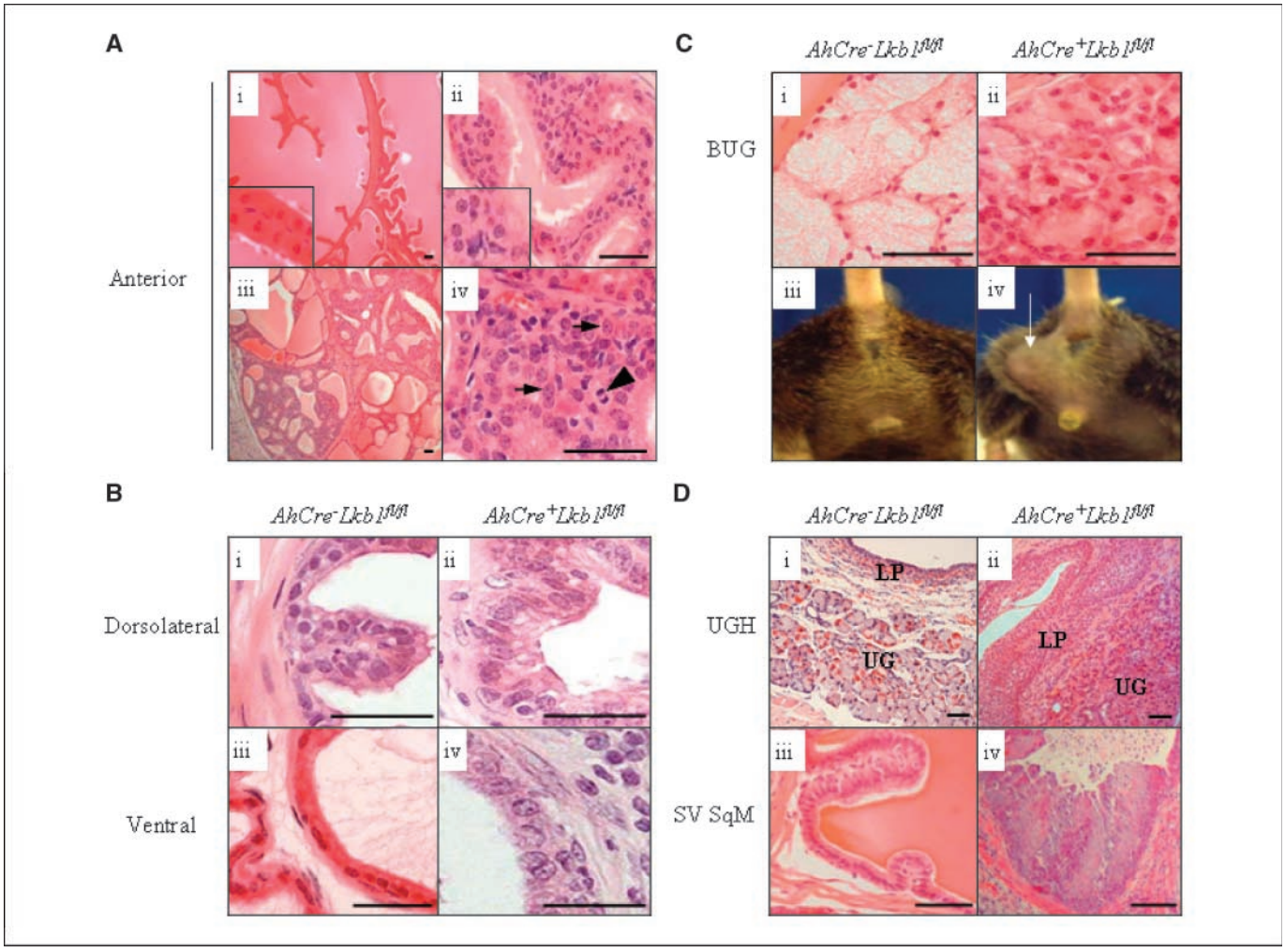

Figure 2. *AhCre*-mediated deletion of *Lkb1* predisposes to multiple GU phenotypes, including PIN. Histologic analysis of H&E sections from *AhCre*$^{-}$*Lkb1*$^{fl/fl}$ and *AhCre*$^{+}$*Lkb1*$^{fl/fl}$ cohorts aged 2 to 7 mo. *A, AhCre*$^{-}$*Lkb1*$^{fl/fl}$ anterior prostate developed normally (*i*). *AhCre*$^{+}$*Lkb1*$^{fl/fl}$ anterior prostate developed AH (*ii*), which progressed to PIN and showed solid and cribriform patterned lesions (*iii*). High power magnification reveals mitotic cells present (*arrow heads*) and nuclear atypia (*arrows*), characteristic of PIN (*iv*). *B, AhCre*$^{+}$*Lkb1*$^{fl/fl}$ dorsolateral and ventral prostate lobes exhibited low-grade hyperplasia in association with nuclear atypia. *C,* the BUG displayed aberrant ductal architecture and chronic infection, suggesting cystic hyperplasia in *AhCre*$^{+}$*Lkb1*$^{fl/fl}$ mice compared with control cohorts (*i–ii*), which were identified by swellings near the base of the tail that developed between 6 and 8 wk (*iii–iv*). *D,* urethral gland and transitional epithelial hyperplasia developed in *Lkb1* mutants, where the lamina propria (*LP*) and urethral glands (*UG*) seem to have proliferated (*i* and *ii*). SV SqM was also observed in *AhCre*$^{+}$*Lkb1*$^{fl/fl}$ mice (*iii* and *iv*). Images were photographed at 20× magnification (low power) or 40× magnification (high power), and scale bars represent 50 μm.

of the GU tract. We assume these other phenotypes prevent progression of PIN to more advanced stages of prostate cancer, such as adenocarcinoma and metastasis. The fact that the *AhCre*$^{+}$*Lkb1*$^{fl/fl}$ lesions are not regenerative and also that not all PIN lesions were associated with inflammation strongly suggests that infection does not drive the development of PIN in this model.

The AhCre transgene mediates recombination in the GU. The observation of a GU phenotype in the *AhCre*$^{+}$*Lkb1*$^{fl/fl}$ mice implied recombination was occurring within these tissues, with subsequent loss of Lkb1 function. To characterize this pattern, we used mice bearing both the *AhCre* transgene and the Rosa26R reporter locus (35). Using this approach, *AhCre*-mediated excision, as reported by LacZ expression, was observed in all four lobes of the prostate and in a mosaic pattern in the urethral glands (Fig. 3*A*). Further LacZ analysis revealed that uninduced *AhCre*-mediated recombination also occurred in the kidney (41), as well as in the BUG, seminal vesicle, testis, epididymis, and vas deferens (not shown). Histologic analysis of the kidney from the *AhCre*$^{+}$*Lkb1*$^{fl/fl}$ cohort determined no abnormalities, whereas the testis, epididymis, and vas deferens showed male hypospermatogenesis and aspermia, respectively. Interestingly, *Lkb1* expression in the testis of *Lkb1*$^{fl/fl}$ hypomorphic male mice is dramatically reduced in the testis. The common 50-kDa isoform is 10-fold lower, whereas the 48-kDa form is completely absent (33).

Recombination of the Lkb1 occurs within the GU and is associated with PIN. To confirm that the Lkb1 kinase domain had been deleted in the neoplastic prostate tissue, LCMD and PCR amplification of extracted DNA samples was carried out. This approach was taken as insufficient tissue was available for Western blots and immunohistochemistry using anti-Lkb1 antibodies did not detect a product in control tissue and was therefore inappropriate to show loss of function. For PCR amplification, positive controls were derived from *AhCre*$^{+}$*Lkb1*$^{fl/fl}$ mice which had been exposed to β-naphthoflavone. This protocol delivers near

100% recombination of the target allele in the liver. Laser capture microdissected DNA from the anterior prostate epithelia of both normal (N) regions from *AhCre$^+$Lkb1$^{fl/fl}$* and *AhCre$^-$Lkb1$^{fl/fl}$* mice served as a negative control for a PCR specific for the recombined *Lkb1* allele (Fig. 3*B*). Semiquantitative densitometry of PIN in the anterior prostate from *AhCre$^+$Lkb1$^{fl/fl}$* mice showed 64% recombination (when compared with fully recombined liver controls). This correlated with a reduction in the level of the unrecombined LoxP-flanked *Lkb1* allele. The fact that recombination was below 100% presumably reflects the observed stromal content in the PIN lesions. These observations establish that recombination of the LoxP-flanked *Lkb1* allele is associated with PIN, but cannot discriminate between loss of function and haploinsufficiency of *Lkb1*.

To confirm depletion of *Lkb1* transcripts in neoplastic tissue, we performed an *in situ* hybridisation specific for *Lkb1* mRNA transcripts. *Lkb1* mRNA was detected in all *wild-type* prostate lobes (ventral prostate not shown) but was not present in *AhCre$^+$Lkb1$^{fl/fl}$* mice (Fig. 3*C*).

Characterization of Lkb1-deficient PIN. To characterize the prostate lesions at a molecular level, immunohistochemistry was performed. The proliferation marker Ki-67 was rarely expressed in control (*AhCre$^-$Lkb1$^{fl/fl}$*) anterior prostate epithelium; however, it was significantly elevated in epithelial cells throughout the acini of *AhCre$^+$Lkb1$^{fl/fl}$* mice (Fig. 4*A*). Basal cells were detected using antibodies against p63 and Keratin-5 in the epithelial lining of anterior acini, indicating a marked accumulation and clustering of

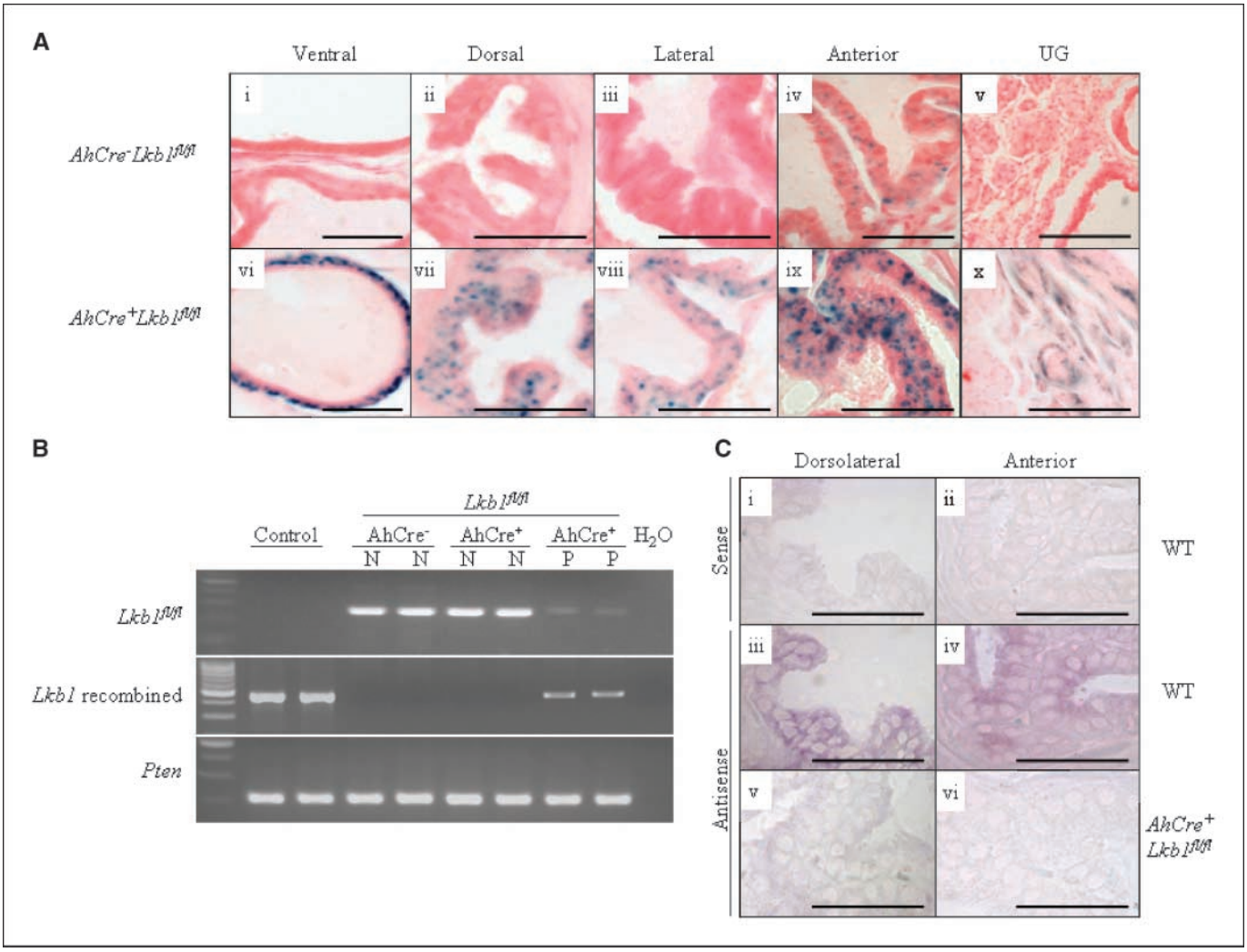

Figure 3. Recombination of *Lkb1* occurs within the GU tract and is associated with PIN. *A,* tissues from adult transgenic mice (ages, 6 mo) were harvested for the detection of Cre recombinase activity using X-gal staining (*blue stain*). Cross-sections of the four individual lobes of the murine prostate (ventral, dorsal, lateral, and anterior) and the urethral glands for *AhCre$^-$Lkb1$^{fl/fl}$* control (*i–v*) and *AhCre$^+$Lkb1$^{fl/fl}$* (*vi–x*) mice. Recombination events were apparent in *AhCre$^+$* tissue after 1 h incubation with the X-gal solution, whereas controls were negative. Some punctate staining was observed in the *AhCre$^-$Lkb1$^{fl/fl}$* anterior prostate, which is attributable to endogenous β-lactamase activity (*iv*). *B,* using LCMD, DNA was isolated from anterior prostate lobes of *AhCre$^-$Lkb1$^{fl/fl}$* ($n = 3$) and *AhCre$^+$Lkb1$^{fl/fl}$* mice ($n = 3$) and underwent PCR analysis. DNA isolated from induced liver tissue from *AhCre$^+$Lkb1$^{fl/fl}$* mice was used as a positive control (near 100% recombination). The top gel represents the unrecombined LoxP-flanked *Lkb1* allele (280 bp), revealing none in the positive control, 100% presence in *AhCre$^-$Lkb1$^{fl/fl}$* and *AhCre$^+$Lkb1$^{fl/fl}$* normal (*N*) samples, and a reduced level of expression in *AhCre$^+$Lkb1$^{fl/fl}$* PIN lesions (*P*). The middle gel refers to *Lkb1* recombined alleles (500 bp), confirming the positive control as ~100% recombined and the *AhCre$^+$Lkb1$^{fl/fl}$* PIN samples partly recombined. Densitometry determined ~64% of *AhCre$^+$Lkb1$^{fl/fl}$* PIN is recombined. *AhCre$^-$Lkb1$^{fl/fl}$* anterior prostate served as a negative control, and the bottom gel depicts *Pten*, used as a loading control (230 bp). *C, in situ* hybridization to detect *Lkb1* mRNA in *wild-type* dorsolateral and anterior prostate lobes determined no unspecific binding using the sense probe (*i* and *ii*), whereas the antisense probe revealed *Lkb1* is expressed in *wild-type* prostate epithelia (*iii* and *iv*). *AhCre$^+$Lkb1$^{fl/fl}$* dorsolateral and anterior prostate lesions show reduced *Lkb1* mRNA transcript levels (*v* and *vi*). Images were taken at 40× magnification, and scale bars represent 50 μm.

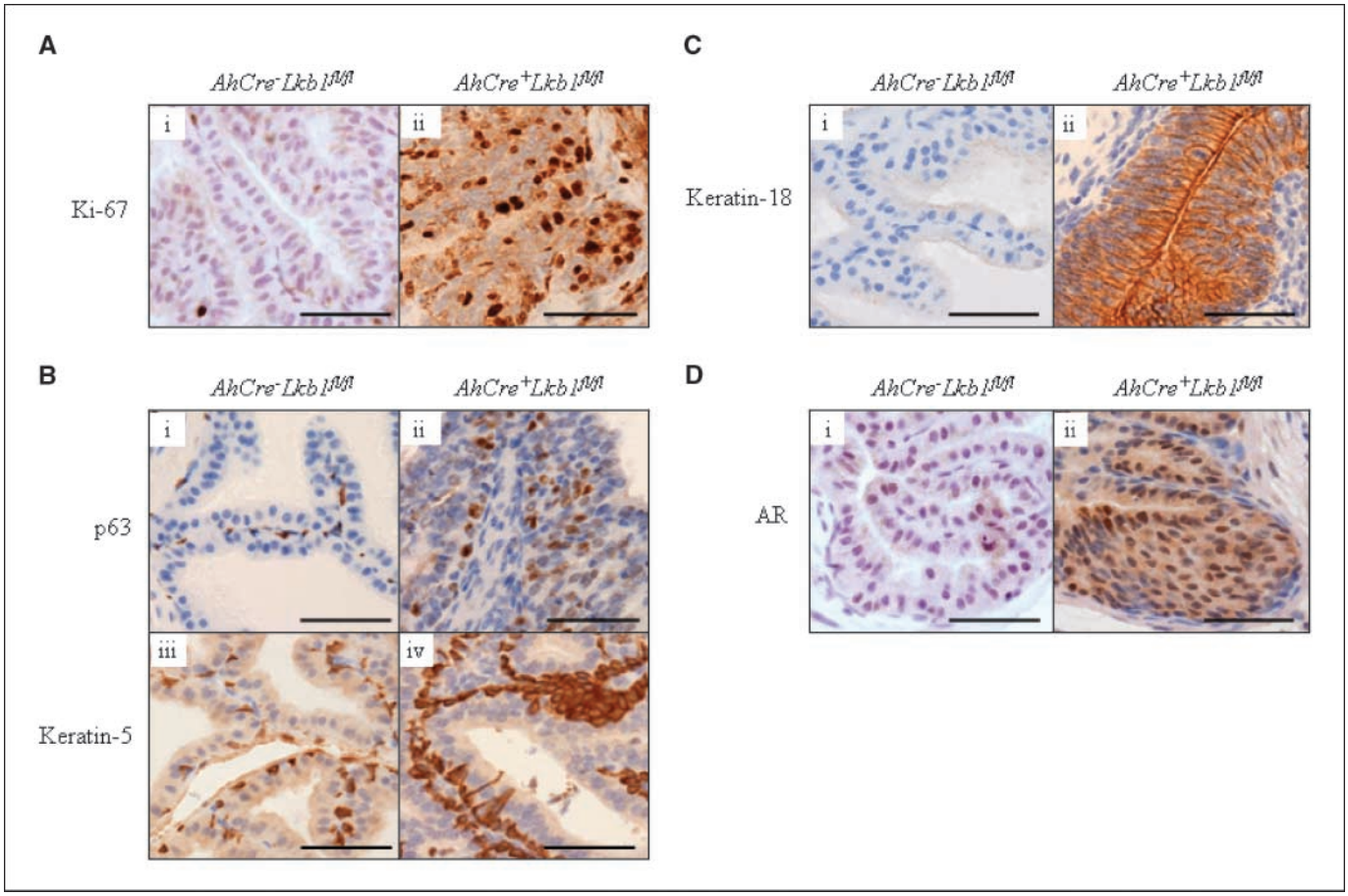

Figure 4. Characterisation of *Lkb1*-deficient PIN. *A,* immunohistochemical analysis of the anterior prostate of control (*AhCre⁻Lkb1$^{fl/fl}$*) and *AhCre⁺Lkb1$^{fl/fl}$* mice (ages 2-7 mo) revealed an increase in proliferation using an anti–Ki-67 antibody. *B,* basal cell clustering was determined by monitoring p63 (*i* and *ii*) and Keratin-5 (*iii* and *iv*) expression. *C,* the luminal cell marker Keratin-18 is elevated in PIN foci. *D,* the androgen receptor (*AR*) is overexpressed in PIN lesions, suggesting deregulation of androgen signaling within neoplastic lesions. Images were taken at 40× magnification, and the scale bars represent 50 μm.

these cells within the lesions (Fig. 4*B*). This pattern of expression was also recently observed in lung tumors from mice bearing *Lkb1* inactivation (12). Keratin-18 is a luminal cell marker. Here, we show an elevation in Keratin-18 expression in PIN foci, mimicking human prostate cancer (Fig. 4*C*). We also show increased expression of the androgen receptor within the lesions, suggesting that PIN development in the context of mutant *Lkb1* is probably androgen sensitive (Fig. 4*D*).

mTOR signaling is decreased in AhCre⁺Lkb1$^{fl/fl}$ PIN after p-AMPK activation. Lkb1 is known to mediate mTOR signaling by the phosphorylation of AMPK under low-energy conditions within the small intestine and skeletal muscle (4, 7, 11, 15). Consequently, in the absence of *Lkb1*, the extent of this phosphorylation event is expected to decrease concomitantly with mTOR signaling activation. To establish on a molecular level whether the loss of *Lkb1* deregulates mTOR signaling in PIN foci, we used immunohistochemistry to stain for active p-AMPKα, p-mTOR, p-S6K (ribosomal protein S6 kinase, 70kDa), an mTOR downstream target, and its substrate p-Rps6 (Fig. 5*A*). We observed an increase in cytoplasmic p-AMPKα expression in association with loss of nuclear p-mTOR in *Lkb1*-deficient PIN lesions, contradicting S6K activation and phosphorylation of its substrate p-Rps6. This suggests that an alternative AMPK kinase (AMPKK) compensates for the absence of *Lkb1*, inhibiting mTOR production and stimulating S6K via an alternative mechanism or that Lkb1 does not regulate AMPK in prostatic epithelia.

Wnt signaling is deregulated in AhCre⁺Lkb1$^{fl/fl}$ PIN. Considering mTOR signaling is not stimulated in *Lkb1*-deficient prostate epithelium, we investigated alternative pathways mediated by Lkb1. To this end, we monitored the expression of a number of Wnt signaling components and downstream transcriptional targets using immunohistochemistry. The β-catenin (CTNNB1) oncogene plays a dual role in cells by participating in both Wnt signaling, essential for normal mammalian development, polarity, and migration, as well as forming adheren junctions at the cell surface membrane together with E-cadherin (42). We observed elevated nuclear β-catenin in PIN foci compared with control tissue, indicating activation of the Wnt signal cascade (Fig. 5*Bi,ii*). Aberrant Wnt signaling was further shown through overexpression of a number of β-catenin transcriptional targets. We detected elevated levels of the migration marker CD44 in PIN foci, a known immediate transcriptional target of Wnt signaling (ref. 43; Fig. 5*Biii,iv*). Foxa1, a Forkhead box factor involved in prostate development and an indirect Wnt target via Sox17 (44), was also up-regulated in PIN lesions (Fig. 5*Bv,vi*). Interestingly, we also observed high-cytoplasmic expression of inactivated p-Gsk3β (Ser^9), a negative regulator of β-catenin (Fig. 5*Bvii,viii*), which further implies perturbation of the Wnt cascade.

Considering the role Lkb1 plays in organizing cellular polarity via Par1A regulation, it is rational for *Lkb1*-deficient prostate epithelial cells to have undergone not only an elevation in Wnt signaling, but also to have lost cell polarity (11, 45). To this end, we analyzed the expression pattern of the tight junction protein ZO-1 using immunofluorescence. This revealed highly organized tight junctions located on the surface of the luminal cells in control tissues. In contrast, *AhCre^{+}Lkb1$^{fl/fl}$* mice showed aberrant expression of ZO-1, being either principally lost completely or perturbed in a small subset of cells. In addition, reduced ZO-1 expression correlated with nuclear accumulation of ZO-1 (Fig. 5*Bix,x*), a phenomenon previously hypothesized to reflect altered regulation of cell polarity events (46).

Deregulation of Pten and Akt in AhCre^{+}Lkb1$^{fl/fl}$ PIN. Recently, Lkb1 has been linked to the Pten/PI3K/Akt pathway (3). To determine whether the PI3K/Akt pathway is deregulated upon loss of *Lkb1*, we used an antibody directed against total Pten (Fig. 6*Ai,ii*) and one that only recognizes inactive/phosphorylated (Ser^{380,385} and Thr^{382}) p-Pten (Fig. 6*Aiii,iv*) to show that inactive Pten is elevated in *Lkb1*-deficient PIN. This suggests loss of Pten function/stability is a direct consequence of losing *Lkb1* function, ultimately facilitating a predisposition to PIN. Lkb1 activation and coincident stabilization of Pten has been shown by *in vitro* studies, supporting our data (3, 23). Consistent with this, the *Lkb1* mutant mice also exhibited increased activation of phosphorylated Akt and the AMPKK p-PDK1 (47) within PIN foci (Fig. 6*Av–viii*). This indicates that the PI3K/Akt pathway is deregulated after *Lkb1* mutation.

Discussion

Murine prostate cancer models are becoming increasingly powerful in elucidating the mechanisms underlying prostate intraepithelial neoplasia, the most established precursor to

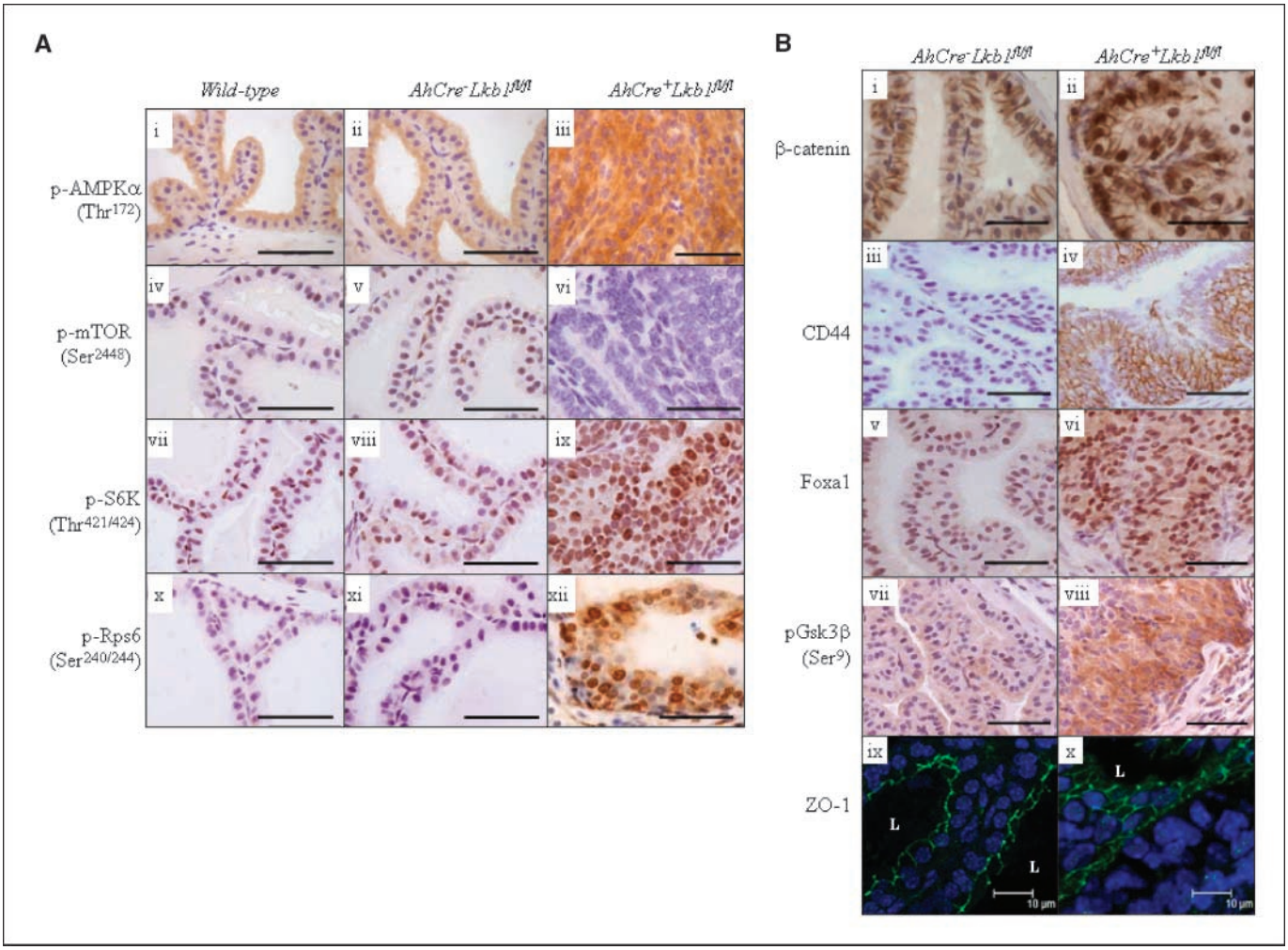

Figure 5. Wnt signaling is activated in *Lkb1*-deficient PIN. *A,* formalin-fixed, paraffin-embedded anterior prostate tissue sections from *AhCre^{-}Lkb1$^{fl/fl}$* and *AhCre^{+}Lkb1$^{fl/fl}$* mice were stained for p-AMPKα (*i–iii*), p-mTOR (*iv–vi*), p-S6K (*vii–ix*), and p-Rps6 (*x–xii*). Within PIN lesions, p-AMPKα expression was elevated throughout the cytoplasm, whereas p-mTOR expression is lost, along with a decrease in mTOR downstream signaling components p-S6K and p-Rps6. Lambda phosphatase treatment was used to determine the extent of any nonspecific staining after anti–p-AMPKα immunohistochemistry, which was observed weakly at the apical surface of the epithelium (as in *i* and *ii*). Similar controls for other antibodies used did not identify any nonspecific staining. *B,* investigations into Wnt signaling components determined that β-catenin (*i* and *ii*), CD44 (*iii* and *iv*), Foxa1 (*v* and *vi*), and p-Gsk3β (*vii* and *viii*) were all elevated in *AhCre^{+}Lkb1$^{fl/fl}$* PIN, indicating Wnt signaling is deregulated. Immunofluorescence for ZO-1 revealed ordered cellular polarity in control mice, whereas cell polarity is disrupted in *AhCre^{+}Lkb1$^{fl/fl}$* PIN foci (*ix* and *x*). ZO-1 exhibited aberrant surface expression and punctate nuclear accumulation. Immunohistochemistry images were taken at 40× magnification, and scale bars represent 50 μm; confocal images were taken at 63× magnification, and scale bars represent 10 μm.

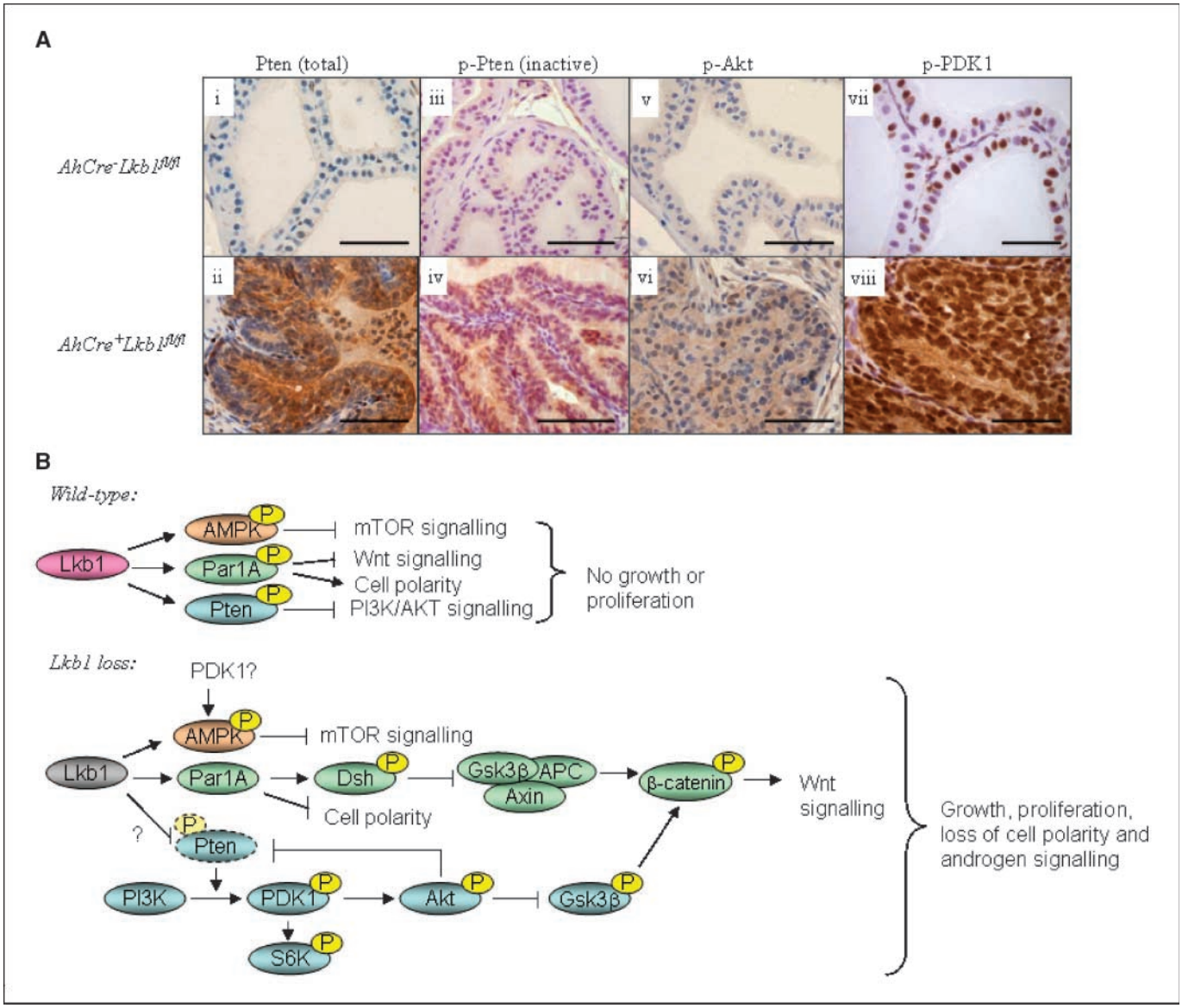

Figure 6. Loss of *Lkb1* stimulates the PI3K/Akt signaling cascade. *A,* immunohistochemistry of control and *AhCre*$^{+}$*Lkb1*$^{fl/fl}$ anterior prostate revealed that total Pten (*i* and *ii*), inactive p-Pten (Ser^{380}/Thr$^{382/383}$; *iii* and *iv*), active phosphorylated Akt kinase (Ser^{473}; *v* and *vi*), and p-PDK1 (Ser^{241}; *vii* and *viii*) are all overexpressed in PIN lesions. Images were taken at 40× magnification, and scale bars represent 50 μm. *B,* a speculative schematic for signaling events mediated by Lkb1 (*top*) and those under *Lkb1* deficient conditions (*bottom*) within prostatic epithelia. Firstly, Lkb1 typically acts to phosphorylate AMPK to suppress mTOR signaling. Once Lkb1 is lost, mTOR signaling may proceed. Our investigations indicate that an alternative AMPK kinase acts on behalf of Lkb1 (e.g., p-PDK1, which stimulates S6K) to sustain mTOR signaling inhibition. Secondly, Lkb1 phosphorylates Par1A to maintain cellular polarity. Upon loss of Lkb1 function, Par1A is redirected to stimulate Disheveled (*Dsh*) to inhibit the APC/Axin/Gsk3β complex, allowing β-catenin to translocate into the nucleus. Here, it stimulates transcription of downstream Wnt target genes and induces growth and proliferation, as well as androgen signaling (51). Finally, although the role of Lkb1 interaction and phosphorylation of Pten is still undefined, our data suggest that Lkb1 maintains Pten stability, inhibiting Akt activation. In the absence of Lkb1, we observed inactivation of Pten function, a common precursor to prostate cancer. Pten loss results in activated Akt and ultimately results in p-Gsk3β expression, which can act to maintain Wnt signaling and drive tumorigenesis.

prostatic carcinoma. Here, we show, for the first time, a role for the tumor suppressor Lkb1 in prostate cancer using Cre-LoxP technology to derive a conditional knockout of *Lkb1* within the prostate epithelial cells. Loss of *Lkb1* reduced male longevity and predisposed to hyperplasia, which progressed to high-grade PIN in the anterior lobe and mild hyperplasia, was also observed in the dorsolateral and ventral glands (within 2–4 months). This positively correlated with β-catenin nuclear translocation and up-regulation of the Wnt and PI3K/Akt signaling cascades within the prostate epithelium. Our immunohistochemical analysis suggests that mTOR signaling seems to decrease after an unexpected surge of p-AMPK in PIN lesions. It is feasible that either Lkb1 does not regulate AMPK within prostate tissue or that an alternative AMPKK compensates for the loss of Lkb1, resulting in suppression of the mTOR pathway. Our data indicate PDK1 is up-regulated in *Lkb1* deficient PIN and may therefore play a role in the observed AMPK phosphorylation and activation of pS6K (47). A speculative schematic of events occurring in the presence and absence of Lkb1 in prostate epithelium is depicted in Fig. 6*B*. One caveat of our studies is that we were limited to immunohistochemical analysis of these proteins, owing to the size of the lesions identified.

Our results from the *AhCre*$^{+}$*Lkb1*$^{fl/fl}$ mice parallel those of previous studies which have monitored the effects of aberrant Wnt signaling in the prostate, demonstrating an association with prostate tumorigenesis (20–22). Upon *Lkb1* loss, Par1A can propagate the translocation of β-catenin into the nucleus to initiate transcription of Wnt target genes, instigating tumorigenesis accompanied with loss of cellular polarity (8). This gives a direct mechanism whereby mutation of *Lkb1* may lead to activated Wnt signaling. The phenotype we observe is somewhat less severe than that reported for either constitutive activation of β-catenin or conditional deletion of *Apc* (20–22). This difference probably reflects differences in gene function (between *Lkb1* and either *Apc* or *β-catenin*) within the prostate, but may also reflect differences in the experimental approaches used, such as the pattern of *Cre*-mediated recombination.

The *Lkb1*-deficient prostate phenotype also parallels the phenotypic characteristics of *Pten*-deficient mice (25–27), although again being somewhat less severe. Loss of *Pten* results in HG-PIN which may progress into carcinoma, where tumorigenesis is positively correlated with the overexpression of p-PDK1, phosphorylated Akt, and its downstream targets, such as pGsk3β (24, 27). *Lkb1* mutant mice paralleled this pattern, and the elevation of both total Pten and inactive Pten was previously observed in the TRAMP model of prostate neoplasia where elevated Pten protein levels, as well as phosphorylation of stabilization sites, associated with inactivation (Ser^{380}, Ser^{385}, and Thr^{382}) correlated with progression (48). Our data therefore suggest loss of *Lkb1* function impairs Pten function, possibly as a consequence of directly interacting and regulating Pten stability (3), leading to enhanced PDK1 and Akt activity, and ultimately predisposing to PIN. This is consistent with an *in vitro* study that speculates LKB1 phosphorylates PTEN to stabilize its function (23). Deregulation of the PI3K/Akt signaling pathway also offers a potential explanation for the observed deregulation of the Wnt pathway via the inactivation of Gsk3β, which maintains Wnt signaling (49, 50).

In summary, we describe here a transgenic mouse model which provides the first link between mutation of the tumor suppressor gene *Lkb1* and prostate neoplasia. Conditional biallelic loss of *Lkb1* leads to the development of a PIN phenotype and to other lesions within the GU. The mechanism underlying this predisposition to PIN involves deregulation of both the Wnt and PI3K/Akt/Pten pathways. Indeed, the phenotype of *Lkb1* deficiency mirrors aspects of both *Pten* loss and Wnt deregulation. Surprisingly, we observed a decrease in mTOR signaling, which we hypothesize may occur as a consequence of a negative feedback mechanism whereby AMPK is activated by an alternate AMPKK to Lkb1, possibly PDK1, to suppress the mTOR pathway. Mechanisms for such deregulation and pathway crosstalk have already been described (Fig. 6*B*), both through the phosphorylation of Par1A and by altering Pten activity/stabilization.

Acknowledgments

Received 8/23/2007; revised 1/15/2008; accepted 1/20/2008.

Grant support: Tenovus (H.B. Pearson).

The costs of publication of this article were defrayed in part by the payment of page charges. This article must therefore be hereby marked *advertisement* in accordance with 18 U.S.C. Section 1734 solely to indicate this fact.

We thank Mark Bishop, Lucie Pietzka, and Derek Scarbrough at Cardiff University for their technical assistance.

References

1. Jemal A, Siegel R, Ward E, et al. Cancer statistics, 2006. CA Cancer J Clin 2006;56:106–30.
2. Chin JL, Reiter RE. Molecular markers and prostate cancer prognosis. Clin Prostate Cancer 2004;3:157–64.
3. Mehenni H, Lin-Marq N, Buchet-Poyau K, et al. LKB1 interacts with and phosphorylates PTEN: a functional link between two proteins involved in cancer predisposing syndromes. Hum Mol Genet 2005;14:2209–19.
4. Yoo LI, Chung DC, Yuan J. LKB1-a master tumour suppressor of the small intestine and beyond. Nat Rev Cancer 2002;2:529–35.
5. Giardiello FM, Welsh SB, Hamilton SR, et al. Increased risk of cancer in the Peutz-Jeghers syndrome. N Engl J Med 1987;316:1511–4.
6. Boardman LA, Thibodeau SN, Schaid DJ, et al. Increased risk for cancer in patients with the Peutz-Jeghers syndrome. Ann Intern Med 1998;128:896–9.
7. Lizcano JM, Goransson O, Toth R, et al. LKB1 is a master kinase that activates 13 kinases of the AMPK subfamily, including MARK/PAR-1. EMBO J 2004;23:833–43.
8. Spicer J, Rayter S, Young N, Elliott R, Ashworth A, Smith D. Regulation of the Wnt signaling component PAR1A by the Peutz-Jeghers syndrome kinase LKB1. Oncogene 2003;22:4752–6.
9. Marignani PA. LKB1, the multitasking tumour suppressor kinase. J Clin Pathol 2005;58:15–9.
10. Alessi DR, Sakamoto K, Bayascas JR. LKB1-dependent signaling pathways. Annu Rev Biochem 2006;75:137–63.
11. Spicer J, Ashworth A. LKB1 kinase: master and commander of metabolism and polarity. Curr Biol 2004;14:R383–5.
12. Ji H, Ramsey MR, Hayes DN, et al. LKB1 modulates lung cancer differentiation and metastasis. Nature 2007;448:807–10.
13. Su G, Hruban R, Bansal R, et al. Germline and somatic mutations of the STK11/LKB1 Peutz-Jeghers gene in pancreatic and biliary cancers. Am J Pathol 1999;154:1835–40.
14. Guldberg P, thor Straten P, Ahrenkiel V, Seremet T, Kirkin A, Zeuthen J. Somatic mutation of the Peutz-Jeghers syndrome gene, LKB1/STK11, in malignant melanoma. Oncogene 1999;18:1777–80.
15. Corradetti MN, Inoki K, Bardeesy N, DePinho RA, Guan KL. Regulation of the TSC pathway by LKB1: evidence of a molecular link between tuberous sclerosis complex and Peutz-Jeghers syndrome. Genes Dev 2004;18:1533–8.
16. Baas AF, Smit L, Clevers H. LKB1 tumor suppressor protein: PARtaker in cell polarity. Trends Cell Biol 2004;14:312–9.
17. Shaw RJ, Bardeesy N, Manning BD, et al. The LKB1 tumor suppressor negatively regulates mTOR signaling. Cancer Cell 2004;6:91–9.
18. Kyriakis JM. At the crossroads: AMP-activated kinase and the LKB1 tumor suppressor link cell proliferation to metabolic regulation. J Biol 2003;2:26.
19. Lee M, Hwang JT, Yun H, et al. Critical roles of AMP-activated protein kinase in the carcinogenic metal-induced expression of VEGF and HIF-1 proteins in DU145 prostate carcinoma. Biochem Pharmacol 2006;72:91–103.
20. Gounari F, Signoretti S, Bronson R, et al. Stabilization of β-catenin induces lesions reminiscent of prostatic intraepithelial neoplasia, but terminal squamous transdifferentiation of other secretory epithelia. Oncogene 2002;21:4099–107.
21. Bierie B, Nozawa M, Renou J, et al. Activation of b-catenin in prostate epithelium induces hyperplasias and squamous transdifferentiation. Oncogene 2003;22:3875–87.
22. Bruxvoort KJ, Charbonneau HM, Giambernardi TA, et al. Inactivation of Apc in the mouse prostate causes prostate carcinoma. Cancer Res 2007;67:2490–6.
23. Song P, Wu Y, Xu J, et al. Reactive nitrogen species induced by hyperglycemia suppresses Akt signaling and triggers apoptosis by upregulating phosphatase PTEN (phosphatase and tensin homologue deleted on chromosome 10) in an LKB1-dependent manner. Circulation 2007;116:1585–95.
24. Trotman LC, Niki M, Dotan ZA, et al. Pten dose dictates cancer progression in the prostate. PLoS Biol 2003;1:E59.
25. Di Cristofano A, Pesce B, Cordon-Cardo C, Pandolfi PP. Pten is essential for embryonic development and tumour suppression. Nat Genet 1998;19:348–55.
26. Di Cristofano A, De Acetis M, Koff A, Cordon-Cardo C, Pandolfi PP. Pten and p27KIP1 cooperate in prostate cancer tumor suppression in the mouse. Nat Genet 2001;27:222–4.
27. Wang S, Gao J, Lei Q, et al. Prostate-specific deletion of the murine Pten tumor suppressor gene leads to metastatic prostate cancer. Cancer Cell 2003;4:209–21.
28. Le Page C, Koumakpayi I, Alam Fahmy M, Mes Masson A, Saad F. Expression and localisation of Akt-1, Akt-2 and Akt-3 correlate with clinical outcome of prostate cancer patients. Br J Cancer 2006;94:1906–12.
29. Conde E, Suarez-Gauthier A, García-García E, et al. Specific pattern of LKB1 and phospho-acetyl-CoA carboxylase protein immunostaining in human normal tissues and lung carcinomas. Hum Pathol 2007;38:1351–60.
30. Collins SP, Reoma JL, Gamm DM, Uhler MD. LKB1, a novel serine/threonine protein kinase and potential tumour suppressor, is phosphorylated by cAMP-dependent protein kinase (PKA) and prenylated *in vivo*. Biochem J 2000;345:673–80.
31. Ikediobi ON, Davies H, Bignell G, et al. Mutation analysis of 24 known cancer genes in the NCI-60 cell line set. Mol Cancer Ther 2006;5:2606–12.
32. Neville P, Conti D, Krumroy L, et al. Prostate cancer aggressiveness locus on chromosome segment 19q12–13.1 identified by linkage and allelic imbalance studies. Genes Chromosomes Cancer 2003;36:332–9.

33. Sakamoto K, McCarthy A, Smith D, et al. Deficiency of LKB1 in skeletal muscle prevents AMPK activation and glucose uptake during contraction. EMBO J 2005;24: 1810–20.

34. Ireland H, Kemp R, Houghton C, et al. Inducible Cre-mediated control of gene expression in the murine gastrointestinal tract: effect of loss of β-catenin. Gastroenterology 2004;126:1236–46.

35. Soriano P. Generalized lacZ expression with the ROSA26 Cre reporter strain. Nat Genet 1999;21:70–1.

36. Shappell SB, Thomas GV, Roberts RL, et al. Prostate pathology of genetically engineered mice: definitions and classification. The consensus report from the Bar Harbor meeting of the Mouse Models of Human Cancer Consortium Prostate Pathology Committee. Cancer Res 2004;64:2270–305.

37. Kikyo N, Williamson CM, John RM, et al. Genetic and functional analysis of neuronatin in mice with maternal or paternal duplication of distal Chr 2. Dev Biol 1997; 190:66–77.

38. Brawer MK. Prostatic Intraepithelial Neoplasia: an overview. Urology 2005;7:S11–8.

39. Bhatia-Gaur R, Donjacour AA, Sciavolino PJ, et al. Roles for Nkx3.1 in prostate development and cancer. Genes Dev 1999;13:966–77.

40. Schneider A, Brand T, Zweigerdt R, Arnold H. Targeted disruption of the Nkx3.1 gene in mice results in morphogenetic defects of minor salivary glands: parallels to glandular duct morphogenesis in prostate. Mech Dev 2000;95:163–74.

41. Sansom O, Griffiths D, Reed KR, Winton D, Clarke A. Apc deficiency predisposes to renal carcinoma in the mouse. Oncogene 2005;24:8205–10.

42. Willert K, Nusse R. β-catenin: a key mediator of Wnt signaling. Curr Opin Genet Dev 1998;8:95–102.

43. Wielenga VJM, Smits R, Korinek V, et al. Expression of CD44 in APC and Tcf mutant mice implies regulation by the WNT pathway. Am J Pathol 1999;154:515–23.

44. Sinner D, Rankin S, Lee M, Zorn AM. Sox17 and β-catenin cooperate to regulate the transcription of endodermal genes. Development 2004;131:3069–80.

45. Forcet C, Etienne-Manneville S, Gaude H, et al. Functional analysis of Peutz-Jeghers mutations reveals that the LKB1 C-terminal region exerts a crucial role in regulating both the AMPK pathway and the cell polarity. Hum Mol Genet 2005;14:1283–92.

46. Gottardi CJ, Arpin M, Fanning AS, Louvard D. The junction-associated protein, zonula occludens-1, localizes to the nucleus before the maturation and during the remodelling of cell-cell contacts. Proc Natl Acad Sci U S A 1996;93:10779–84.

47. Bayascas JR, Leslie NR, Parsons R, Fleming S, Alessi DR. Hypomorphic mutation of PDK1 suppresses tumorigenesis in PTEN (+/-) mice. Curr Biol 2005;15:1839–46.

48. Shukla S, Maclennan GT, Marengo SR, Resnick MI, Gupta S. Constitutive activation of PI3K-Akt and NF-kB during prostate cancer progression in autochthonous transgenic mouse model. Prostate 2005;64: 224–39.

49. Green JB. Lkb1 and GSK3-β: kinases at the center and poles of the action. Cell Cycle 2004;3:12–4.

50. Al-Khouri AM, Ma Y, Togo SH, Williams S, Mustelin T. Cooperative phosphorylation of the tumor suppressor phosphatase and tensin homologue (PTEN) by casein kinases and glycogen synthase kinase 3β. J Biol Chem 2005;280:35195–202.

51. Yardy GW, Brewster SF. Wnt signaling and prostate cancer. Prostate Cancer Prostatic Dis 2005;8:119–26.